Effects of Poly(vinyl acetate) and Poly(vinyl chloride-*co*-vinyl acetate) Low-Profile Additives on Properties of Cured Unsaturated Polyester Resins. I. Volume Shrinkage Characteristics and Internal Pigmentability

Yan-Jyi Huang, Tzong-Shyang Chen, Jyh-Gau Huang, Fuh-Huah Lee

Department of Chemical Engineering, National Taiwan University of Science and Technology, Taipei, Taiwan 106, Republic of China

Received 29 May 2002; accepted 4 December 2002

ABSTRACT: Three series of self-synthesized poly(vinyl acetate)-based low-profile additives (LPAs) with different chemical structures and molecular weights, including poly(vinyl acetate), poly(vinyl chloride-*co*-vinyl acetate), and poly(vinyl chloride-*co*-vinyl acetate-*co*-maleic anhydride), were studied. Their effects on the volume shrinkage characteristics and internal pigmentability for low-shrink unsaturated polyester (UP) resins during cure were investigated. The experimental results were examined with an integrated approach involving measurements of the static phase characteristics of the ternary styrene/UP/LPA system, the reaction kinetics, the cured sample morphology, and microvoid formation by using differential scanning calorimetry, scanning electron microscopy, optical microscopy, and image analysis. Based on the Takayanagi mechanical model, factors leading to both good volume shrinkage control and acceptable internal pigmentability for the molded parts were explored. © 2003 Wiley Periodicals, Inc. J Appl Polym Sci 89: 3336–3346, 2003

Key words: unsaturated polyester resin; low-profile additives; curing; volume shrinkage; internal pigmentability

INTRODUCTION

Adding specific thermoplastic polymers as low-profile additives (LPA) into unsaturated polyester (UP) resins can lead to the reduction or even elimination of polymerization shrinkage during the cure process.[1,2] However, when low-profile polyester molding compounds, such as low-profile bulk molding and sheet molding compounds, are formulated with pigments, they may exhibit unacceptable haziness of the pigment's color. In general, the better the shrinkage control for the LPA, the poorer the internal pigmentation in terms of color depth. Recently, unique LPAs have been developed[3] that give significantly improved deep color pigmentation with modified polyester resins while maintaining a smooth surface and zero shrinkage, yet the fundamental principle involved has not been examined.

Depending on the chemical composition and structure of the UP resins and LPA that are employed, differing degrees of drift in the styrene (St)/UP/LPA composition, which is a result of phase separation during cure, may occur for the St/UP/LPA system.[4–7] This can lead to various cured sample morphologies and different crosslinking densities among the phase regions, and it may greatly affect the physical and mechanical properties of cured samples.[8–13] It has been reported that[6] the static ternary phase characteristics at 25°C for St/UP/LPA may be employed as a rough guide for explaining the observed morphology during the reaction at 110°C, where a flakelike or globule microstructure in either the continuous or dispersed phase can arise. After phase equilibrium at 25°C for St/UP/LPA systems, the upper layer (i.e., the dispersed phase) was generally dominated by St and LPA whereas the bottom layer (i.e., the continuous phase) was dominated by UP and St. The molar ratio of St/polyester C═C bonds in the upper layer was greater than that in the original mixture, and the trend was reversed in the bottom layer.

The objective of this work is to investigate the effects of poly(vinyl acetate) (PVAc) and vinyl chloride-VAc copolymer (VC-VAc) based LPAs on the volume shrinkage characteristics and internal pigmentability for St/UP/LPA ternary systems using an integrated approach combining measurements for the static phase characteristics of the ternary St/UP/LPA system, the reaction kinetics, the cured sample morphology, and property measurements. A mechanism is proposed that leads to both good volume shrinkage

Correspondence to: Y.-J. Huang (HUANGYJ@mail.ntust.edu.tw).

Contract grant sponsor: National Science Council of the Republic of China; contract grant number: NSC 87-2216-E-011-010.

Journal of Applied Polymer Science, Vol. 89, 3336–3346 (2003)

TABLE I
Raw Materials Used in Synthesis of Three Selected LPAs

LPA Codes	VCM	VAc	MA	LPO	Trichloroethylene[a]	Methyl Cellulose[b]	H_2O
PVAc3S	—	100 g (1.16)	—	1.5 g (3.76×10^{-3})	1.5 g (0.011)	2.5 g	400 g
VC-VAc2S	100 g (1.6)	20.58 g (0.239)	—	0.1808 g (4.53×10^{-4})	3.978 g (0.0302)	0.723 g	483 g
VC-VAc-MA1S	84 g (1.344)	16 g (0.185)	5 g (0.051)	0.4 g (10^{-3})	0.8 g (6.08×10^{-3})	0.723 g	400 g

VCM, vinyl chloride monomer; LPO, lauroyl peroxide, an initiator. The values in parentheses are in moles.
[a] A chain transfer agent.
[b] A suspending agent.

control and acceptable internal pigmentability for the molded parts.

EXPERIMENTAL

Synthesis of PVAc-based LPA

The PVAc-based LPAs employed with different chemical structures and molecular weights were synthesized by suspension polymerizations in a 2-L stainless steel stirred reactor (model 4522, Parr) at 60–75°C for 6–13 h.[14,15] The weight ratio of water/monomer was kept at 4:1, and the stirring speed was maintained at 420 rpm. Lauroyl peroxide (Aldrich), trichloroethylene (Acros), and methyl cellulose with a number-average molecular weight (M_n) of 14,000 g/mol (Acros) were used as the initiator, chain-transfer agent, and suspending agent, respectively. The first series of LPAs was made from VAc (Acros); the second series was made from VC (Fluka) and VAc; and the third series was made from VC, VAc, and maleic anhyride (MA, Acros). Eight LPAs were synthesized, and the raw materials used in the synthesis of the three LPAs selected for this study are summarized in Table I.

For the synthesis of the PVAc homopolymer, deionized water was first degased at 95°C for 1 h and then introduced into the reactor after cooling. Distilled VAc monomer, initiator, and chain transfer agent were placed in a 250-mL beaker and mixed at room temperature by magnetic stirring (mixture A). Mixture A and a suspending agent were then fed into the reactor. After the reactor was sealed, a nitrogen sparge for the reactor was started and maintained for 15 min, followed by stirring for 20–25 min to obtain a uniform suspension of monomer in the water. The reactant was then polymerized at 65°C for 3 h and reacted at 75°C for another 3 h. After it was cooled to room temperature, the product slurry was taken out of the reactor, washed with deionized water several times, filtered, dried at room temperature for 24 h, and stored for further characterization and use.

A semibatch process was adopted for copolymer synthesis because of its better control of copolymer composition. For the synthesis of the VC-VAc random copolymer as an LPA, degased deionized water, mixture A, and suspending agent were introduced into the reactor first. The procedure that was used was the same as described above except that the final reactant temperature was lowered to 10°C to facilitate the subsequent feeding of VC monomer (VCM) into the reactor. In order to introduce VCM into the reactor, a three-way valve was used to transfer it (gas state, bp −14°C, mp −154°C) from the original bottle to a stainless steel cooling coil (with the other end connected to a feeding valve and the reactor) immersed in a Dewar flask filled with liquid nitrogen. With the stirring in the reactor turned off, the liquid VCM in the coils was subsequently pumped into the reactor by nitrogen gas via the three-way valve. The VCM (74 g) and nitrogen gas were pumped into the reactor until a 150 psig level was reached. The stirring in the reactor was restarted and maintained for 30 min to allow sufficient suspension of VCM in water. The reactant was then raised to 60°C for polymerization. After a 2.5-h reaction time, 8.4 g of VCM was introduced into the reactor by following the procedures mentioned above. Three additional feedings of VCM were conducted at 45-min intervals with feed amounts of 7, 6, and 4.6 g. After the last feeding of VCM, the polymerization at 60°C was continued for 7.75 h. The total reaction time was 12.5 h before the reaction was terminated. After it was cooled to room temperature, the product slurry was taken out of the reactor, precipitated with methyl alcohol, washed with deionized water several times, filtered, dried in a vacuum oven at 40°C for 24 h, and stored for further characterization and use.

For the synthesis of VC-VAc-MA random terpolymer as an LPA, the procedure was essentially the same as that for VC-VAc except for the following points. First, mixture A now contained MA in addition to VAc, initiator, and chain transfer agent. Second, 37.5 g of VCM was first pumped into the reactor, followed by nitrogen gas until a 105 psig level was reached. For the first 5 h of reaction time, another 28.5 g of VCM was introduced into the reactor by adding 5.7 g/h. For the subsequent 2.5 h of reaction time, the other 18 g of VCM was introduced into the reactor at 6 g every 50 min. After the last feeding of VCM, the polymerization at 60°C was continued for 3.5 h. The total reaction time was 11 h before the reaction was terminated.

TABLE II
LPAs Used in Study

LPA Codes	Monomer	Molar Compos.[a]	M_n[b]	M_w[b]	PD[b]	T_g(°C)[c]
PVAc1S	VAc	—	23,000	53,000	2.30	24.1
PVAc2S	VAc	—	83,000	131,000	1.58	23.6
PVAc3S	VAc	—	109,000	166,000	1.52	20.4
VC-VAc1S	VC, VAc	0.85:0.15	34,000	54,000	1.59	56.8
VC-VAc2S	VC, VAc	0.858:0.142	39,000	61,000	1.56	61.0
VC-VAc3S	VC, VAc	0.878:0.122	50,000	75,000	1.50	63.0
VC-VAc4S	VC, VAc	0.874:0.126	71,000	93,000	1.31	65.4
VC-VAc-MA1S	VC, VAc, MA	0.829:0.159:0.011	60,000	81,000	1.35	67.5

[a] Determined by ^{1}H-NMR.
[b] Determined by GPC (g/mol)
[c] Determined by DSC.

The properties of the three series of LPAs in this study (PVAc, VC-VAc, and VC-VAc-MA) are summarized in Table II.

UP resins

The UP resin[7] was made from MA, 1,2-propylene glycol (PG), and phthalic anhydride with a molar ratio (MR) of 0.63:1.01:0.367. The acid and hydroxyl numbers were found to be 28.0 and 28.2, respectively, by end-group titration, which gives an M_n of 2000 g/mol. On average, the calculated number of C═C bonds in each polyester molecule was 6.79.

Preparation of sample solutions

For the sample solution, 10 wt % LPA was added and the MR of St/polyester C═C bonds was fixed at 2/1. The reaction was initiated by 1 wt % *tert*-butyl perbenzoate. For the sample solution with pigment, 10 wt % Bordeaux Red was added as pigment, which had irregular shape and nonuniform size distributions centered at 0.5–3 and 5–6 μm.

Phase characteristics

To study the compatibility of St/UP/LPA systems prior to reaction, 20 g of sample solutions were prepared in 100-mL separatory glass cylinders, which were placed in a 25°C constant-temperature water bath. The phase separation time was recorded, and the mixture of each layer was separated and weighed.

Cure kinetics

For the cure kinetic study, 6–10 mg of sample solution was placed in a hermetic aluminum sample pan. The isothermal reaction rate profile at 110°C was measured by a DuPont 9000 differential scanning calorimeter, and the final conversion of total C═C bonds was calculated.[16]

Scanning electron microscopy (SEM)

In the morphological study, the fractured surface of the sample, which was cured at 110°C for 1 h and postcured at 150°C for 1 h in a stainless steel mold, was observed by SEM at 1000×.

Microvoids

The morphology of the sample during cure was also observed by means of an optical microscope. One drop of sample (~0.8 mg) was placed between two microscope cover glasses, which were then inserted into a hot stage microscope (FP82HT, Mettler). The cured sample at 110°C was chilled in liquid nitrogen and subsequently observed at room temperature under an optical microscope using transmitted light at magnifications of 100–400×.

The quantity of microcracking in the morphology sample under optical microscopy was measured by means of an image analyzer.[17,18] Because the samples were of uniform thickness, the fraction of the image area that was black (because of light scattering by the microcracks) was proportional to the volume of the microcracks in the sample.

Volume change and calorimetric measurements

Density measurements[18] at room temperature were employed to obtain the volume shrinkage data for isothermally cured specimens at 110°C. The measurements of the color depth[19] at room temperature for the corresponding cured specimens were carried out by using a chromameter (CR-300, Minolta). Ten measurements of the L^* value as a color depth index were taken for both sides of the specimen. With a higher L^* value, the color depth is lower and the hazing phenomenon of the cured specimen is more pronounced, because of worse internal pigmentability. In this study, an L^* value of 30 was recognizably dark red in

TABLE III
Calculated Molar Volumes and Dipole Moments for UP and LPA and Phase Separation Time for St/UP/LPA Uncured Systems at 25°C

	μ[a]	V[b]	μ'[c]	$\mu'_{UP} - \mu'_{LPA}$	t_p[d]
UP resin					
MA-PG-PA	3.13	1,389	0.084		—
LPA					
PVAc1S	10.63	17,810	0.080	0.004	∞[e]
PVAc2S	20.18	64,280	0.080	0.004	∞
PVAc3S	23.13	84,410	0.080	0.004	∞
VC-VAc1S	10.48	22,060	0.071	0.013	∞
VC-VAc2S	11.20	25,790	0.070	0.014	∞
VC-VAc3S	12.72	32,100	0.071	0.013	5[f]
VC-VAc4S	15.43	47,590	0.071	0.013	3[g]
VC-VAc-MA1S	14.42	39,390	0.073	0.011	∞

[a] Dipole moment ($D/mol^{1/2}$).
[b] Molar volume (cm^3/mol).
[c] Dipole moment per unit volume [$=(\mu^2/V)^{1/2}$; $D/cm^{3/2}$].
[d] Phase separation time (min) at 25°C.
[e] One phase.
[f] 17.0% by weight for the upper layer solution.
[g] 56.4% by weight for the upper layer solution.

tint and it can be considered as the acceptable upper bound for good internal pigmentability.

RESULTS AND DISCUSSION

Synthesis of PVAc-based LPA

For the VC-VAc copolymer, the introduction of VAc can alter the glass-transition temperature (T_g) and molecular polarity in comparison with poly(VC) (T_g = 78°C). This may then change the miscibility of the St/UP/LPA ternary system. For the VC-VAc-MA copolymer, the introduction of MA can facilitate the reaction of the carboxylic acid group in MA with a thickening agent, such as MgO, during the thickening[20] process in the preparation of polyester molding compounds. Hence, the phase separation of LPA from the molding compound can be prevented prior to the cure reaction.

Characterization of LPA

The molar compositions of VC-VAc and VC-VAc-MA types of LPAs shown in Table II were identified by ^{1}H-NMR, where the peak intensities of —CH_2 (δ = 2.2–2.4) and —CH— (δ = 4.3–4.6) for both VC and VAc, —CH_3 for VAc (δ = 2.2), and $>$CH— for MA (δ = 3.7) were selected for the calculations. (Simultaneous equations were solved because of the peak overlap.)

The M_n values measured by gel permeation chromatography for the eight PVAc-based LPAs fell in the range of 23,000–109,000 g/mol, and the polydispersity ranged from 1.3 to 2.3 (Table II).

The differential scanning calorimetry (DSC) results in Table II show that the T_g values for PVAc, VC-VAc, and VC-VAc-MA are 20–25, 57–65, and 68°C, respectively. The introduction of VC or MA monomer into the PVAc backbone can lead to an increase of the stiffness of polymer chain and, in turn, to an increase in the T_g.

Compatibility of St/UP/LPA ternary systems prior to cure

The molecular polarity of the UP resin and LPA was evaluated in terms of the calculated dipole moment per unit volume[7] ($\mu/V^{1/2}$) by using the Debye equation[21] and group contribution methods.[21,22] In general, the higher the polarity difference per unit volume between UP and LPA ($\mu_{UP}' - \mu_{LPA}'$), the less is the compatibility for the St/UP/LPA system at 25°C prior to the reaction. The data in Table III reveal that the sample solution containing PVAc is theoretically the most compatible, followed by the VC-VAc-MA and VC-VAc systems. This is in agreement with the data of the phase separation time in Table III, where the VC-VAc system is the only one with phase separation occurring at 25°C prior to the reaction.

Cured sample morphology, cure kinetics, and compatibility of cured St/UP/LPA ternary systems

During the cure at 110°C, the sample solution containing PVAc was also the most compatible, followed by the VC-VAc-MA and VC-VAc systems. This is evidenced by the cured sample morphology for the fractured surface [compare Fig. 1(a–h)] and the final conversion of the total C═C bonds (see Fig. 2). The most compatible PVAc system exhibited a homogeneous globule cured morphology containing a continuous

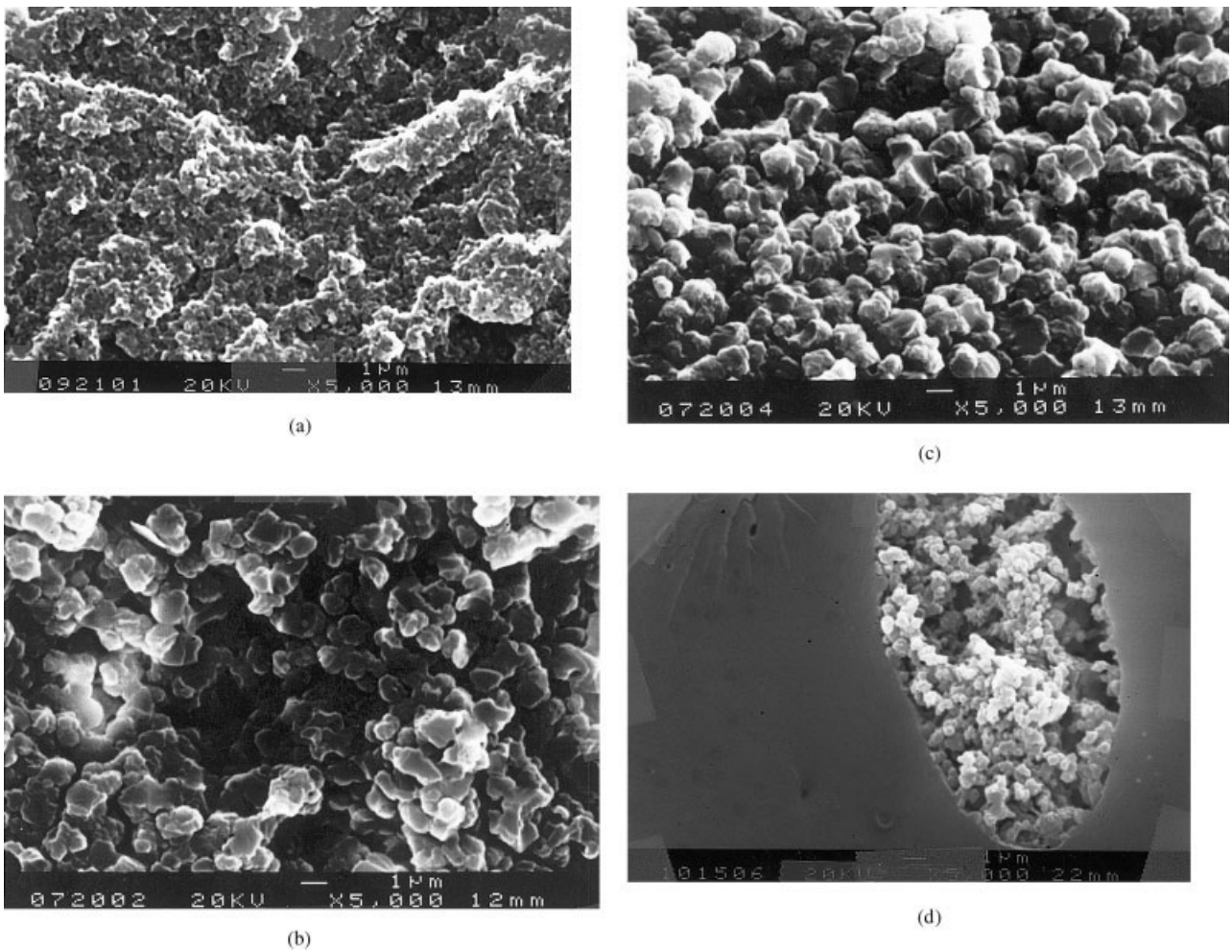

Figure 1 The effects of the LPA types on the cured sample morphology under SEM for (a) PVAc1S, (b) PVAc2S, (c) PVAc3S, (d) VC-VAc1S, (e) VC-VAc2S, (f) VC-VAc3S, (g) VC-VAc4S, and (h) VC-VAc-MA1S.

St-crosslinked polyester phase (i.e., microgel particle) and a cocontinuous LPA-rich phase [Fig. 1(a–c)]. The least compatible VC-VAc system exhibited a two-phase microstructure consisting of a flakelike continuous phase and a globule LPA-dispersed phase [Fig. 1(d–g)]. In contrast, the VC-VAc-MA system possessed a two-phase microstructure but with a much smaller domain size of the globule LPA-dispersed phase than those of the VC-VAc systems [compare Fig. 1(h) and (d–g)], indicating that the VC-VAc-MA system was more compatible than the VC-VAc one.

Moreover, the final conversion of total C═C bonds was generally the highest for the most compatible PVAc system, followed by VC-VAc-MA and VC-VAc. This is ascribed to the fact that the MR of St/polyester C═C bonds in the major continuous phase of the St-crosslinked polyester would have less deviation from an MR of <2:1 for the more compatible St/UP/LPA system during the cure. A better St swelling effect on the microgel structure in the major continuous phase could lead to a higher final cure conversion[16] therein, and, in turn, a higher overall cure conversion.

As expected, adding a higher molecular weight of LPA caused less compatibility of the St/UP/LPA system during the cure because the phase separation was more noticeable. This was evidenced by the more pronounced microgel particle precipitation for the less compatible PVAc systems [compare Fig. 1(a–c), where the PVAc3S system was the least compatible] and the larger average area of the LPA-dispersed phase for the more incompatible VC-VAc system [compare Fig. 1(d–g), where the VC-VAc4S system was the most incompatible].

For both the PVAc and VC-VAc systems, increasing the LPA molecular weight may result in a higher final conversion of total C═C bonds, yet further increases of the LPA molecular weight (i.e., the PVAc3S system) can lead to a remarkable reduction in the final conversion [Fig. 2(b)]. Increasing the LPA molecular weight could lead to an increase in both the phase separation time (because of the increase of the solution viscosity) and the degree of phase separation (because of the decrease of the change in entropy in the solution process) prior to gelation during the cure, both of which

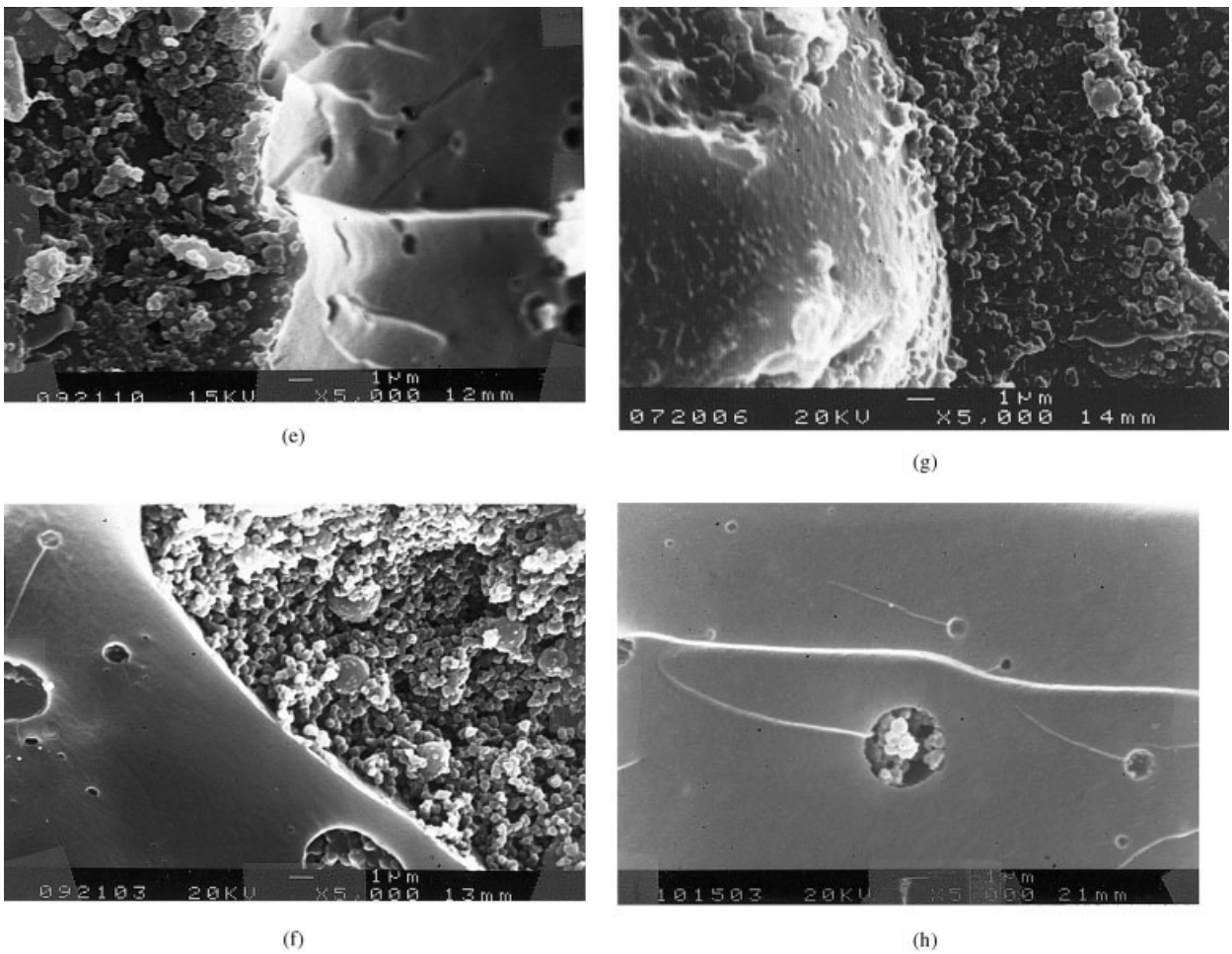

Figure 1 (*Continued from the previous page*)

may affect the dynamic phase characteristics of St/UP/LPA systems, such as the ternary compositions among the phases. The later phase separation time (or lower phase separation rate) is favorable for the increase of final conversion because the MR of St/polyester C═C bonds in the major continuous phase of St-crosslinked polyester would deviate less from an MR of <2:1 and can thus enhance the final cure conversion as mentioned earlier.[16] In contrast, the higher degree of phase separation is unfavorable for the increase of the final conversion because the MR in the major continuous phase of the St-crosslinked polyester would deviate more a from an MR of <2:1. Apparently, for the PVAc3S system, the adverse effect of the degree of phase separation would be much more significant than the favorable effect of the phase separation time caused by the greater increase in the LPA molecular weight, which leads to a noticeable reduction in the final cure conversion.

As pointed out in our previous work,[12] the relative magnitude of the peak reaction rate in the DSC rate profile can be employed as an index for the degree of phase separation during the cure. In general, a less compatible ternary system is evidenced by a relatively lower peak reaction rate. However, only the DSC peak reaction rate data [Fig. 2(a)] for the PVAc systems were in accord with the trend of compatibility of cured St/UP/LPA systems as revealed by the SEM micrographs in Figure 1 (i.e., PVAc1S > PVAc2S > PVAc3S).

Takayanagi models

For the cured LPA-containing UP resin systems with the morphologies shown in Figure 1(a–h), their mechanical behavior can be approximately represented by the Takayanagi models,[23,24] in which arrays of weak LPA (R phase) and stiff St-crosslinked polyester (P phase) phases are indicated (see Fig. 3). The subscripts 1, 2, and 3 for the P phases are employed because of the distinction of St and UP compositions as a result of phase separation during cure. The quantities λ, ϕ, ξ, and ν or their indicated multiplications indicate the volume fractions of each phase.

For the systems shown in Figure 1(a–c), the microgel particles (P_1 phase) are surrounded by a layer of

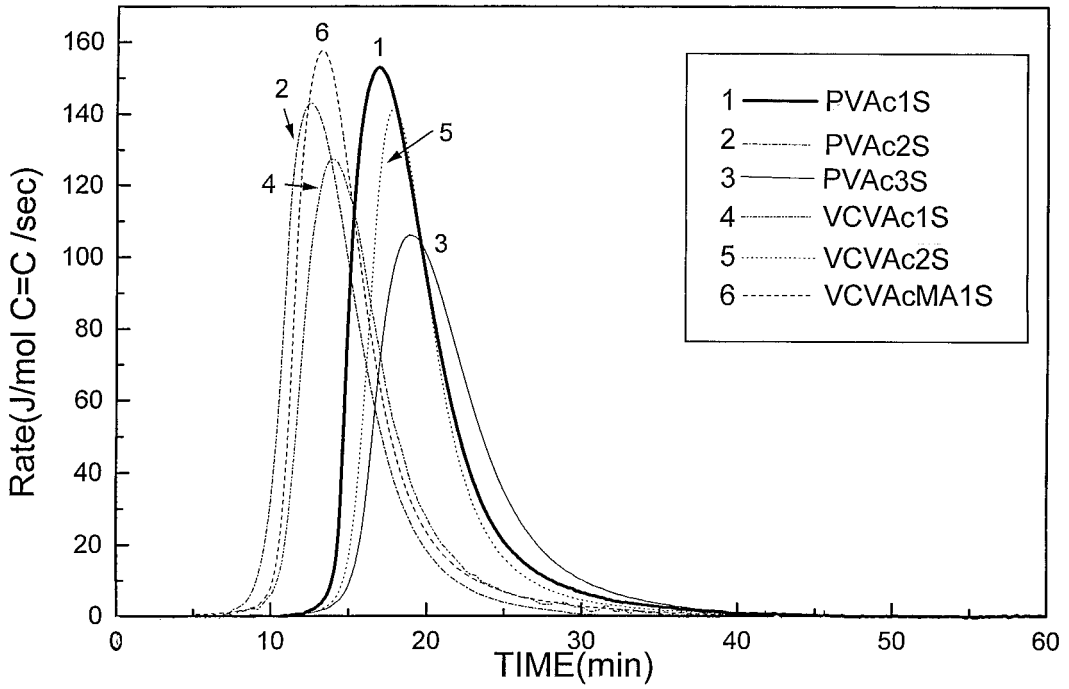

(a)

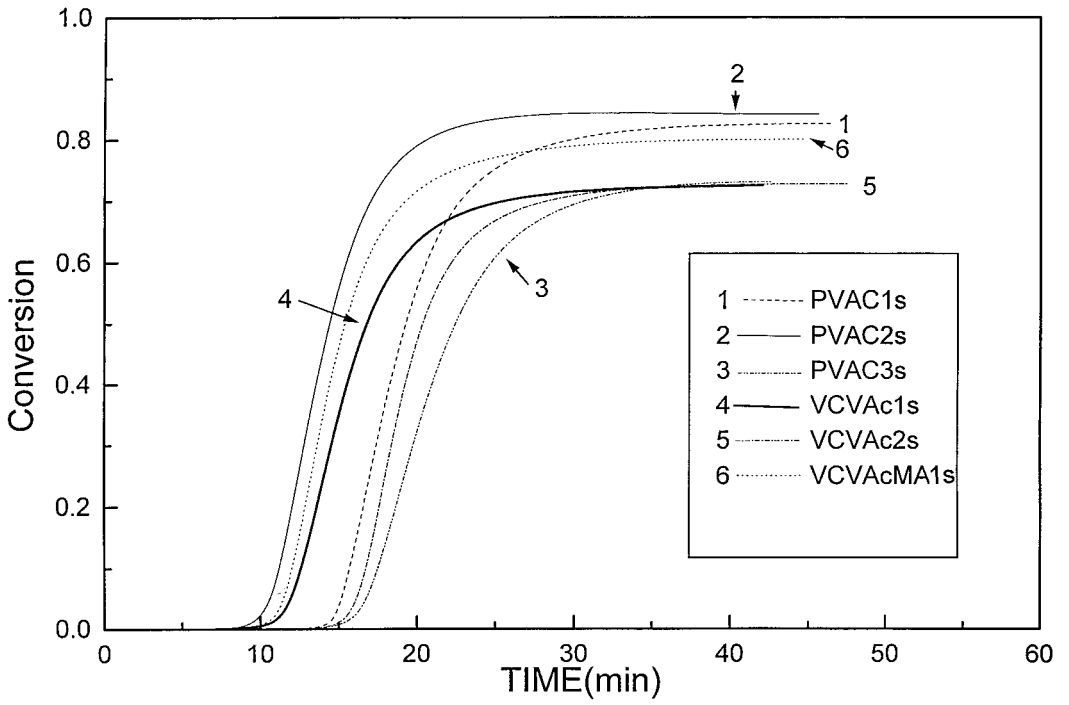

(b)

Figure 2 (a) The effects of the LPA types on the DSC reaction rate profile at 110°C for St/UP/LPA systems and (b) the corresponding cure conversion profiles of total C═C bonds as measured by DSC. The final cure conversion for the neat UP resin at MR = 2/1 is 91.8%.

LPA (R phase). Between the LPA-covered microgel particles there are some lightly St-crosslinked polyester chains and polystyrene chains (taken together as the P_2 phase), which have different compositions of St and UP than those in the P_1 phase, that are dispersed in the LPA phase (R phase). Hence, the characteristic globule microstructure may be represented by the parallel-parallel-series (P-P-S) model as shown in Figure 3(a), which is a parallel combination of the three elements (P_1, R, and P_2-R) in series. In contrast, for the

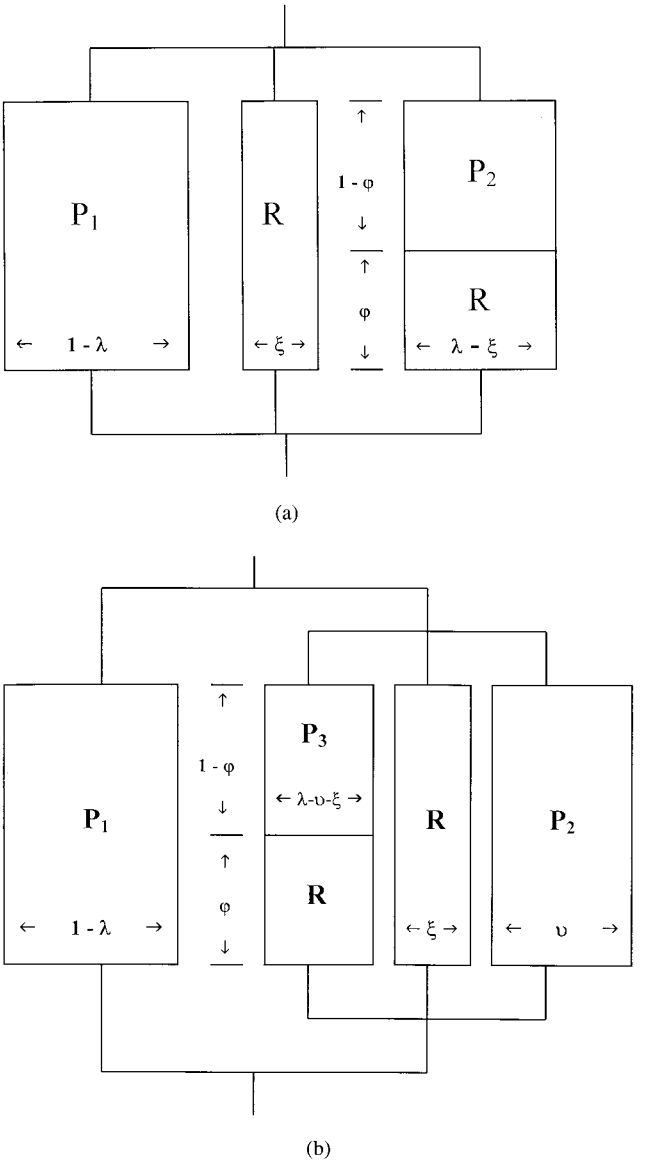

Figure 3 The Takayanagi models: (a) parallel-parallel-series (P-P-S) and (b) parallel-parallel-parallel-series [P-(P-P-S)]. The area of each diagram is proportional to a volume fraction of the phase.

system shown in Figure 1(d–h), the microstructure consists of a stiff continuous phase of St-crosslinked polyester (phase P_1) and a weak globule LPA-dispersed phase, whose globule morphology can also be represented by a P-P-S model. Hence, the upper bound of mechanical behavior for the overall morphology can be represented by a parallel- parallel-parallel-series [P-(P-P-S)] model as shown in Figure 3(b), which is simply a parallel combination of the continuous phase P_1 and the dispersed phase denoted by a P-P-S model.

Volume shrinkage and internal pigmentability

The volume shrinkage of the neat UP resin was about 8%, but adding different PVAc-based LPAs can reduce the volume shrinkage to about 2–7% (Table IV). The most compatible PVAc system would generally be the most effective for volume shrinkage control, followed by the VC-VAc and VC-VAc-MA systems. In addition, the higher the molecular weight for LPA, the better the volume shrinkage control.

The effects of the LPA chemical structure and molecular weight on the L^* value as the index of internal pigmentability for St/UP/LPA systems after the cure generally shows a trend that is the reverse of those on the fractional volume shrinkage. Based on the tint in the upper side of the molded parts, the performance of the internal pigmentability was better for the less compatible VC-VAc and VC-VAc-MA systems compared to the more compatible PVAc systems. Because an L^* value of 30 can be employed as the acceptable upper bound for good internal pigmentability, all of the systems except the PVAc2S system exhibit good internal pigmentability (Table IV).

Effects of microvoid formation and intrinsic polymerization on volume shrinkage

Pattison et al.[25,26] have proposed that, as the crosslinking of LPA-containing UP resins proceeds, strain due to polymerization shrinkage develops in the system,

TABLE IV
Volume Shrinkage Data ($\Delta V/V_0$) L^* Value as Index of Internal Pigmentability for Both Sides of Molded Parts, and Volume Fraction of Microvoids (v_m) for St/UP/LPA Systems after Isothermal Cure at 110°C

LPA Added	$\Delta V/V_0$ (%)	L^* (Upper Side)	L^* (Bottom Side)	v_m (%)
Neat Resin	−7.88	22.24 (0.03)[a]	23.08 (0.06)	—
PVAc1S	−6.24	29.59 (0.13)	29.05 (0.11)	3.56
PVAc2S	−3.68	56.07 (0.26)	45.32 (0.21)	13.87
PVAc3S	−2.14	24.94 (0.06)	24.93 (0.08)	48.97
VC-VAc1S	−6.75	23.56 (0.10)	23.14 (0.04)	2.21
VC-VAc2S	−6.56	23.14 (0.05)	23.68 (0.03)	2.58
VC-VAc3S	−6.10	—	—	—
VC-VAc4S	−5.90	24.31 (0.10)	24.60 (0.07)	10.16
VC-VAc-MA1S	−7.20	21.43 (0.05)	24.76 (0.12)	12.77

* The values in parentheses represent the estimated standard errors for the experimental averages.

particularly at the interface of LPA phase and crosslinked UP phase. This strain can increase to the point that stress cracking propagates through the weak LPA phase, relieving this strain, forming microcracks and/or microvoids, and compensating for the overall volume shrinkage by the microcrack or microvoid space.

Table IV shows the relative volume fraction of microvoids (v_m) for various St/UP/LPA systems. The volume fraction of microvoids was generally the highest for the most compatible PVAc system, followed by the VC-VAc-MA and VC-VAc systems. In addition, the higher the molecular weight for LPA, the higher was the volume fraction of microvoids. Therefore, greater microvoid formation may generally give less volume shrinkage, which generally supports the volume shrinkage mechanism of strain relief through stress cracking.

Besides microvoid formation, intrinsic polymerization shrinkage[18] can also affect the fractional volume shrinkage after cure. The worst volume shrinkage control for the VC-VAc-MA system is attributable to the relatively high cure conversion (compare Fig. 2 and Table IV).

Effects of microvoid formation on internal pigmentability

Atkins and Rex[3] pointed out that microvoid formation is also intimately connected with the internal pigmentability of molded parts. As incident light enters an internally pigmented part of the cured St/UP/LPA system, the intensity of reflective light to the pigment can be greatly reduced because of the severe light scattering that may occur at the solid/air (microvoid) and UP/LPA interfaces inside the parts, leading to haziness of the pigment color. Because the difference in the refractive index between the solid/air interface of a microvoid and that of UP/LPA is approximately 0.5 and 0.07, respectively, the dominant factor in the haziness of pigment color is the presence of microvoids. (The refractive indices for air, UP, and PVAc are 1.00, 1.54, and 1.47, respectively, as reported by Atkins and Rex.)

According to the Lorentz and Lorenz formula,[21] the refractive index (n_D) can be calculated as follows:

$$n_D = [(1 + 2R_{LL}/V)/(1 - R_{LL}/V)]^{1/2} \qquad (1)$$

where R_{LL} is the molar refraction and V is the molar volume. Based on the group contribution method, the R_{LL} of a species can be calculated by $R_{LL} = \Sigma R_{LLi}$, where R_{LLi} is the constitution unit i for that species. The calculated refractive indices for the UP resin and LPAs are displayed in Table V, where the difference in the refractive index between UP and air is about 2–5 times larger than that of UP and LPA (0.59 vs. 0.12–0.37).

TABLE V
Calculated Refractive Index (n_D) for UP and LPA

LPA	n_D	n_D (UP) − n_D
UP resin		
MA-PG-PA	1.587	0
LPA		
PVAc	1.467	0.120
VC-VAc	1.339	0.248
VC-VAc-MA	1.221	0.366
PS	1.603	−0.016
Others		
Air	1.000	0.587

PS, polystyrene.

In general, the higher the volume fraction of microvoids (PVAc > VC-VAc-MA > VC-VAc), the worse the internal pigmentability in terms of more pigment hazing, as revealed by a higher L^* value on the upper side of molded parts (Table IV). However, the L^* value for the PVAc3S system was ≤30, despite its highest volume fraction of microvoids, which is in contrast to that for the PVAc2S system ($L^* \gg 30$), even with a relatively lower volume fraction of microvoids.

Factors in good volume shrinkage control and acceptable internal pigmentability

Among the eight St/UP/LPA systems, the PVAc3S system provided good volume shrinkage control ($\Delta V/V_0 \cong -2.1\%$) and achieved acceptable internal pigmentability ($L^* \cong 25.0$). The relatively higher volume fraction of microvoids (≈49%) can lead to better volume shrinkage control. Nevertheless, it is inferred that the average size of the microvoids should be smaller than 0.05–0.1 μm, which is about 1/10 to 1/5 of the wavelength of visible light (wavelength of visible light = 0.45–0.75 μm), so that the light scattering caused by the high volume fraction of microvoids would be insignificant and the haziness of a pigment's color could be minimized.

Factors in microvoid formation

Microvoids and microcracks essentially exist in the phase region with a cocontinuous globule microstructure, where the interface generated between the LPA-rich phase and the crosslinked UP phase makes possible strain relief through stress cracking and the subsequent formation of microvoids and microcracks in the weak LPA-rich phase. Therefore, the volume fraction of microvoids generated during the cure of the St/UP/LPA system may depend upon three factors: the polymerization strain in the crosslinked polyester phases (ϵ_{Pi}), the interfacial area (A_i) between the LPA-rich phase (phase R in Fig. 3) and the crosslinked UP

TABLE VI
Factors Affecting Volume Fraction of Microvoids (v_m) and Average Size of Microvoids (s_m) for St/UP/LPA System During Cure

Factors	MR_{Pi}	Y_{Pi}	MR_R	ϵ_{YR}	A_i	ϵ_{Pi}	v_m	s_m
1. Cured sample morphology								
(a) Cocontinuous globule morphology					↑[a]		↑	
(b) Two-phase microstructure					↓[b]		↓	
2. Degree of reaction-induced phase separation								
(a) Higher MW of LPA					↑		↑	
(b) Higher MW of LPA	↓	↑				↓	↓	↓
(c) Higher MW of LPA			↑	↓			↑	↓
(d) Higher MW of LPA				↓			↑	↓
3. Stiffness of UP resin								
(a) MA-PG type of UP		↓				↑	↑	↑
(b) MA-PG-PA type of UP		↑				↓	↓	↓
4. T_g of LPA								
(a) Lower T_g of LPA				↓			↑	↓
5. Cure temp.								
(a) Higher cure temp.				↓			↑	↓

[a] Increase.
[b] Decrease.

phase (phases P_1, P_2, and P_3 in Fig. 3), and the yield strain for the LPA-rich phase (ϵ_{YR}). In contrast, the average size of the microvoids (s_m) may depend upon two factors, namely, ϵ_{Pi} and ϵ_{YR}.

The ϵ_{Pi} value can be controlled by the Young's modulus in the crosslinked polyester phases (Y_{Pi}), which may depend upon the chain stiffness of the UP resin employed and the MR of St/polyester C═C bonds reacting in the crosslinked polyester phases as a result of reaction-induced phase separation during the cure (MR_{Pi}). The A_i value can be controlled by the cured sample morphology and the degree of phase separation during the cure and, in turn, the compatibility of the uncured St/UP/LPA system. The ϵ_{YR} can be controlled by the temperature difference between the T_g of the LPA employed and the cure temperature (ΔT), the LPA concentration, and the MR in the LPA-rich phase (MR_R) as a result of reaction-induced phase separation during the cure. The effects of the cured sample morphology, degree of reaction-induced phase separation, stiffness of the UP resin, the T_g of the LPA, and the cure temperature on v_m and s_m values are summarized in Table VI.

In this work, the St/UP/PVAc cured system exhibited a cocontinuous globule microstructure, which is favorable for the increase of A_i and the enhancement of v_m. On the other hand, employing an MA-PG-PA type of UP resin, instead of MA-PG type, can increase Y_{Pi}, leading to a reduction in the ϵ_{Pi}. This in turn may result in a decrease in the v_m and a reduction in the s_m. Moreover, employing a higher molecular weight LPA, such as PVAc3S, can enhance reaction-induced phase separation during the cure, leading to a lower MR_{Pi}, a higher MR_R, and a higher LPA concentration in the LPA-rich phase. The higher degree of phase separation during cure may increase the A_i and v_m; the lower MR_{Pi} may lead to a higher Y_{Pi} and a lower ϵ_{Pi}, and, in turn, a reduction in both v_m and s_m. The higher MR_R may cause a lower ϵ_{YR}, an increase in v_m, and a decrease in s_m. The higher LPA concentration in the LPA-rich phase may result in a lower ϵ_{YR}, an increase in v_m, and a decrease in s_m. In addition, employing a relatively lower T_g LPA in reference to the cure temperature (110°C in this study), such as PVAc (T_g = 20–24°C), may decrease the ϵ_{YR} and can lead to a higher v_m and a lower s_m (Table VI).

To sum our findings, employing the MA-PG-PA type of UP resin, a higher molecular weight LPA, and a relatively lower T_g LPA may all result in a reduction of the s_m (Table VI), which is favorable for acceptable internal pigmentability. Although employing the MA-PG-PA type of UP resin may decrease the v_m (Table VI), which is unfavorable for volume shrinkage control, yet employing a higher molecular weight LPA and a relatively lower T_g LPA may both lead to an increase in the v_m (Table VI). This can compensate for decreases in the v_m that are due to the use of the MA-PG-PA type of UP resin. Consequently, good volume shrinkage control can still be achieved.

CONCLUSIONS

The effects of PVAc-based LPAs with different chemical structures and molecular weights on the volume shrinkage characteristics and internal pigmentability for St/UP/LPA systems were investigated by an integrated approach of the static phase characteristics, cured sample morphology, reaction kinetics, microvoid formation, and property measurements. Based on the Takayanagi mechanical model, factors leading to both good volume shrinkage control and acceptable

internal pigmentability for the molded parts were discussed.

Microvoid formation during the cure of St/UP/LPA systems is closely connected with not only the volume shrinkage control but also the internal pigmentability. A higher volume fraction of microvoids can generally lead to better volume shrinkage control but more haziness of pigment color. The volume fraction of microvoids may depend on the polymerization strain in the densely crosslinked polyester phases, the interfacial area between the crosslinked polyester phase and the LPA-rich phase, and the yield strain of the LPA-rich phase. The first factor can be controlled by the stiffness of the UP resin that is employed; the second factor can be controlled by the cured sample morphology and, in turn, the compatibility of the uncured St/UP/LPA system; and the third factor can be influenced by the glass-transition temperature of the LPA that is used. A cocontinuous globule cured sample morphology, which can lead to the generation of sufficient interfacial area between the densely crosslinked polyester phase and the LPA-rich phase during the cure, lower stiffness of the UP resin, and lower T_g for the LPA in reference to the cure temperature, can result in a higher volume fraction of microvoids and microcracks generated during the cure.

For the St/UP/LPA system during the cure, by controlling the average size of microvoids down to about 1/10 to 1/5 of the wavelength of visible light, the higher volume fraction of such microvoids can still result in both good volume shrinkage control and acceptable internal pigmentability. The average size of the microvoids generated during the cure may generally depend upon both the polymerization strain in the crosslinked polyester phases and the yield strain of the LPA-rich phase. The lower the polymerization strain in the crosslinked polyester phases developed by employing a higher stiffness UP resin or the lower the yield strain in the LPA-rich phase by employing a lower T_g LPA in reference to the cure temperature, the smaller the average size of the microvoids is. Employing an MA-PG-PA type of UP resin (MA/PA MR $\cong$ 0.63:0.37) and a PVAc3S type of LPA (M_n = 109,000 g/mol, T_g = 20°C) in this study allowed us to achieve good volume shrinkage ($\Delta V/V_0 = -2.1\%$) and acceptable internal pigmentability ($L^* \cong 25.0$)

The financial support of this work by the National Science Council of the Republic of China is greatly appreciated.

References

1. Bartkus, E. J.; Kroekel, C. H. Appl Polym Symp 1970, 15, 113.
2. Atkins, K. E. In Sheet Molding Compounds: Science and Technology; Kia, H. G., Ed.; Hanser: New York, 1993; Chapter 4.
3. Atkins, K. E.; Rex, G. C. In 48th Annual Conference; Composites Institute; The Society of the Plastics Industry (SPI), Eds.: Washington, DC, 1993; p 6-D.
4. Suspene, L.; Fourquier, D.; Yang, Y. S. Polymer 1991, 32, 1593.
5. Hsu, C. P.; Kinkelaar, M.; Hu, P.; Lee, L. J. Polym Eng Sci 1991, 31, 1450.
6. Huang, Y. J.; Su, C. C. J Appl Polym Sci 1995, 55, 323.
7. Huang, Y. J.; Jiang, W. C. Polymer 1998, 39, 6631.
8. Lam, P. W. K. Polym Eng Sci 1989, 29, 690.
9. Bucknall, C. B.; Partridge, I. K.; Phillips, M. J. Polymer 1991, 32, 786.
10. Park, M. B. C.; Mcgarry, F. J. In 48th Annual Conference; Composites Institute; The Society of the Plastics Industry (SPI), Eds.: Washington, DC, 1993; p 10B.
11. Huang, Y. J.; Chen, L. D. Polymer 1998, 39, 7049.
12. Huang, Y. J.; Chu, C. J.; Dong, J. P. J Appl Polym Sci 2000, 78, 543.
13. Huang, Y. J.; Lee, S. C.; Dong, J. P. J Appl Polym Sci 2000, 78, 558.
14. Chen, T. S. M.S. Thesis, National Taiwan University of Science and Technology, 1998.
15. Sorenson, W. R.; Campbell, T. W. Preparative Methods of Polymer Chemistry, 2nd ed.; Interscience: New York, 1968; p 229.
16. Huang, Y. J.; Su, C. C. J Appl Polym Sci 1995, 55, 305.
17. Mitani, T.; Shiraishi, H.; Honda, K.; Owen, G. E. In 44th Annual Conference; Composites Institute; The Society of the Plastics Industry (SPI), Eds.: Washington, DC, 1989; p 12F.
18. Huang, Y. J.; Liang, C. M. Polymer 1996, 37, 401.
19. Atkins, K. E.; Rex, G. C.; Reid, C. G.; Seats, R. L.; Candy, R. C. In 47th Annual Conference; Composites Institute; The Society of the Plastics Industry (SPI), Eds.: Washington, DC, 1992; p 7-D.
20. Huang, Y. J.; Wen, Y. S. Polymer 1994, 35, 5259.
21. (a) Van Krevelen, D. W. Properties of Polymers, 3rd ed.; Elsevier: London, 1990; p 198; (b) Van Krevelen, D. W. Properties of Polymers, 3rd ed.; Elsevier: London, 1990; p 292; (c) Van Krevelen, D. W. Properties of Polymers, 3rd ed.; Elsevier: London, 1990; p 323.
22. Fedors, R. F. Polym Eng Sci 1974, 14, 147.
23. Takayanagi, M.; Imada, K.; Kajiyama, T. J Polym Sci Part C Polym Chem 1966, 15, 263.
24. Huang, Y. J.; Horng, J. C. Polymer 1998, 39, 3683.
25. Pattison, V. A.; Hindersinn, R. R.; Schwartz, W. T. J Appl Polym Sci 1974, 18, 2763.
26. Pattison, V. A.; Hindersinn, R. R.; Schwartz, W. T. J Appl Polym Sci 1975, 19, 3045.